Erosion Prediction in Ungauged Basins: Integrating Methods and Techniques (Proceedings of symposium HS01 held during IUGG2003 at Sapporo, July 2003). IAHS Publ. no. 279, 2003.

Reliability evaluation of rainfall–sediment–runoff models

TAKAHIRO SAYAMA
Graduate School of Civil Engineering, Kyoto University, Sakyo-ku, Kyoto 606-8501, Japan
sayama@rdp.dpri.kyoto-u.ac.jp

KAORU TAKARA, YASUTO TACHIKAWA
Disaster Prevention Research Institute, Kyoto University & CREST, JST, Uji, Kyoto 611-0011, Japan

Abstract This paper proposes a method of evaluating model reliability based on a Monte Carlo simulation technique, and applies it to distributed rainfall–sediment–runoff models with different complexity in the rainfall–runoff processes. The proposed evaluation method indicates that the model dealing with subsurface flow and surface flow is the most reliable among the three models for the Lesti River basin, for which hourly rainfall discharge sequences are available. By using the evaluated rainfall–runoff process models, sediment erosion and transportation in the Lesti River basin are simulated.

Key words distributed rainfall–sediment–runoff model; model reliability; Monte Carlo simulation; optimum model complexity

INTRODUCTION

The circulation of water and sediment is an important aspect of environmental problems in river basins. Accurate prediction of sediment transport in river basins by using a relevant model is becoming very important for integrated water and sediment management. However, we often face the problem of inadequate, unreliable data, especially in the case of sediment. It is therefore important to investigate the reliability of simulation results with the limited data available, and to use a model that maximizes the reliability, depending on the data availability.

This paper proposes a method to evaluate model reliability by using a Monte Carlo simulation technique. The method clearly shows the reliability of simulation results, even when a rainfall–runoff model is applied to an ungauged basin. The optimum model complexity depends on data availability and purposes. It should be evaluated in terms of not only the best performance for the calibration period, but also in terms of model reliability.

THE EVALUATION OF MODEL RELIABILITY FOR AN UNGAUGED BASIN AND A GAUGED BASIN

The evaluation involves the following steps:
(a) A generic form of a rainfall–runoff model is described as:

$$q_i = f_i(x, r, \theta) \tag{1}$$

where q_i is the output of model i, x is a state vector, r is an input vector, θ is a parameter vector (p-dimensional), and f_i is the structure of model i. Suppose that there are alternative models $i \in [1, n]$. A parameter vector is selected from a feasible parameter set S_f:

$$\theta \in S_f \tag{2}$$

We have an infinite combination of parameters $\theta_1, \theta_2, ..., \theta_p$ for model i. For ungauged basins, the optimum parameter values for each parameter vector cannot be specified. Therefore, generating $\theta_1, \theta_2, ..., \theta_p$ by a Monte Carlo approach would be justified.

(b) Generate M parameter vectors for each model.

(c) Using a parameter vector and given input variables, we simulate the hydrograph, and compare it with observation to obtain an evaluation index (EI) such that:

$$EI = G\left[f_i(x, r_o, \theta), q_o\right] \tag{3}$$

where r_o is observed rainfall, q_o is observed discharge, and G is the operation between observed discharge and model output sequences. Note that observed discharge data are not available in an ungauged basin. However, this procedure assumes that the performance of a model is similar in basins where hydro-climatic conditions are similar, and investigates model reliability in the different basins where discharge data are available.

(d) Repeat step (c) M times.

(e) Graph the distribution of EI (see Fig. 1).

(f) We define the probability of exceeding a particular threshold EI_* as the model reliability for ungauged basins α_{ung}.

$$\alpha_{ung}(EI_*) = \mathrm{Prob}(EI \geq EI_*) \tag{4}$$

For example, in Fig. 1, the reliability of Model 1 and Model 2 are 80% and 20%, respectively. Model 1 therefore would be used for other ungauged basins in similar hydro-climatic conditions as a model with a reliability of 80% under the condition of $EI \geq EI_*$.

(g) For a gauged basin, calibrated parameter vectors that satisfy EI_* with observed data q_o and r_o can be used for applications. A calibrated parameter set S_c and a calibrated parameter vector θ_c are expressed by equation (5):

$$\theta_c \in S_c$$
$$S_c = \left[\theta \mid G\left[f_i(x, r_o, \theta), q_o\right] \geq EI_*\right] \tag{5}$$

(h) Using the calibrated parameter vector θ_c and given input for a validation period, we simulate the hydrograph, and compare it with observations to obtain an evaluation index for validation period (EI_v).

(i) Graph the distribution of EI_v.

(j) We define the probability of exceeding a particular threshold EI_{v*} as the model reliability for gauged basins as follows:

$$\alpha_{gag}(EI_{v*}) = \text{Prob}(EI_v \geq EI_{v*}) \tag{6}$$

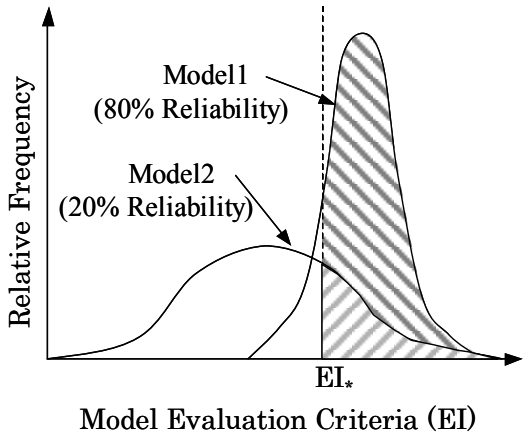

Fig. 1 The schematic diagram of model reliability.

DISTRIBUTED RAINFALL–SEDIMENT–RUNOFF MODEL

Saturated and unsaturated flow in rainfall–runoff processes

The model simulates saturated and unsaturated flow in its rainfall–runoff processes. The Field Capacity model is combined with the surface-subsurface Kinematic Wave Runoff (KWR) model given by equations (7) and (8) (Shiiba *et al.*, 1998):

$$\frac{\partial h}{\partial t} + \frac{\partial q}{\partial x} = r_e(x,t) \tag{7}$$

$$q = \begin{cases} d_c k_c \left(\dfrac{h}{d_c}\right)^{\beta} i & 0 \leq h \leq d_c \\ (h - d_c) k_s i + d_c k_c i & d_c < h \leq d_s \\ \dfrac{\sqrt{i}}{n}(h - d_s)^m + (h - d_c) k_s i + d_c k_c i & d_s < h \end{cases} \tag{8}$$

where q is discharge per unit width, h is water depth, d_c is equivalent depth for field capacity, d_s is depth of the subsurface layer, k_s is the hydraulic conductivity of the subsurface layer, $k_c(d_c/h)^{\beta}$ is the hydraulic conductivity for the unsaturated layer, i is the slope, n is the Manning coefficient, and m is 5/3.

Sediment yield and deposit process model on slope cells

The grid-cell-based KWR model (Kojima, 1997) simulates rainfall–runoff on each grid-cell, and has the same resolution as the Digital Elevation Model (DEM). The sediment yield and deposit process model assumes that sediment transport takes place when surface flow occurs. The model considers the transport capacity of surface flow on each grid-cell for each time step to model erosion as well as deposition. The

transport capacity is calculated by equation (9), which is based on the Unit Stream Power (USP) theory (Yang, 1996). The grid-cell-based KWR model simulates the mean velocity V and the discharge Q on each grid-cell for each time step. Transport capacity (TC) is the product of the C_t and Q as in equation (10):

$$\log C_t = I + J\left(\frac{VS}{\omega} - \frac{V_{cr}S}{\omega}\right) \tag{9}$$

$$TC = C_t Q \tag{10}$$

If the volume of sediment supplied by upstream grid-cells (Q_{sin}) is bigger than the TC, the volume of sediment of $TC - SI$ will be yielded. On the other hand, the sediment from the upstream grid-cells will be deposited, with a volume of $SI - TC$, when SI is bigger than TC because surface flow cannot move all of the sediment (Moore & Burch, 1986).

Sediment transport model in river channels

A single channel is taken into account in each grid-cell of the "River" land-cover class. The channel width is decided by regime theory. The sediment that reaches the "River" grid-cell is transported downstream in the channel as bed load and suspended load. The bed load is computed with the equation proposed by Ashida & Michiue (1972), and the suspended load with the equation proposed by Lane & Kalinske (1941).

APPLICATION TO THE LESTI RIVER BASIN, INDONESIA

The Lesti River basin

The model was applied to the Lesti River basin (625 km^2), located in the upper Brantas River basin (12 000 km^2), which is the second largest river on Java, Indonesia. The Lesti River basin is covered with volcanic soil because of the eruption of Mt Semeru. The Senggruh Dam, which is located at the junction of the Lesti River and the Brantas River, was constructed in 1988 for water resources management and power generation. At present, 85% of its gross storage volume (21.5 million m^3) has been filled with sediment. Sedimentation at the Senggruh Dam and in the river channels is one of the major causes for decreasing the dam's lifetime and increasing the risk of flooding. Prediction of sediment movement at the drainage basin scale is the most important task before planning any mitigation measures.

Spatial information

Data sets of geographic information such as flow direction, slope and land cover on each grid-cell are needed to develop distributed hydrological models. In Indonesia, however, DEMs and recent land-use maps are not available. To overcome this

problem, this research project involves the use of GIS to generate a DEM, and remote sensing to classify land cover. After digitizing contour lines on a 1:50 000 topographic map of the area of interest, a Triangulated Irregular Network (TIN) was generated and transformed into a 250-m resolution DEM. An ADEOS/AVNIR image (NASDA, 1997), acquired on 4 June 1997 with a spatial resolution of 16 m, was used to make a land-cover classification map using a maximum likelihood classifier. Each grid-cell is assigned a Manning coefficient based on the land-cover class.

Optimum model complexity in terms of model reliability

By using the proposed evaluation method of model reliability, we estimate the reliability of three models with different model complexities to find the optimum model complexity for the Lesti River basin in terms of the reliability.

The rainfall–runoff models to be investigated are described by equations (7) and (8). The field capacity model simulates rainfall–runoff processes in detail. This complex model accounts for surface flow, subsurface flow and field capacity, and is referred to as Model 3. Setting d_c to zero simplifies the model by not considering the field capacity, and this model configuration is referred to as Model 2. Likewise, by setting d_s to zero, the model simulates only surface flow, and this model configuration is referred to as Model 1. Thus, model complexity can be changed by varying the parameters.

In addition, a feasible parameter set S_f for each model must be selected. Table 1 shows the feasible model parameter ranges for the Lesti River basin. The complex model (Model 3) requires more parameters than the simple models (Models 1 and 2). In this paper, only the Manning coefficient is spatially distributed according to the land cover, whereas other parameters are spatially uniform over the basin. The Manning coefficient for a model run is the product of a random factor from the feasible range and the Manning coefficient of the land-cover class.

A uniform independent random sampling procedure is applied to select each parameter value to generate a parameter vector for each simulation, and the model simulates sediment–rainfall–runoff with 200 randomly generated parameter vectors. By using hourly rainfall and discharge data observed in the Lesti River basin from 4–6 December 1995, we simulate the hydrograph with the parameter vector. In this research, the Nash–Sutcliffe efficiency (Nash & Sutcliffe, 1970) is used as an evaluation index. This step was repeated 200 times.

Figure 2 shows frequency distributions of the Nash–Sutcliffe efficiency (EFF) calculated using the three models. According to Fig. 2, Model 1 seems to be more

Table 1 Feasible ranges of parameters for the three models for the Lesti River basin.

	Factors for the Manning coefficient *	Hydraulic conductivity ($m\ s^{-1}$)	Depth of A layer (m)	Porosity for field capacity	Beta ($= KK_c^{-1}$)
Model 1	0.1–1.0				
Model 2	0.1–1.0	0.01–0.1	0–0.5		
Model 3	0.1–1.0	0.01–0.1	0–0.5	0–0.3	2–3

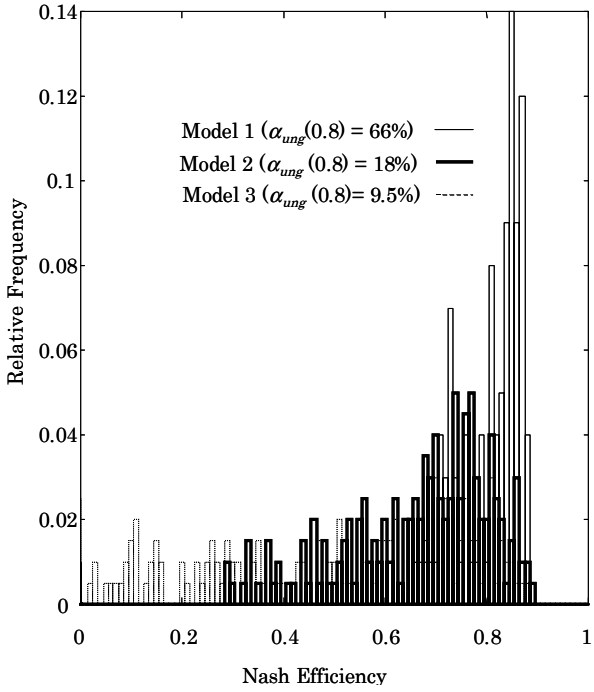

Fig. 2 Frequency distribution of Nash–Sutcliffe Efficiency for the calibration.

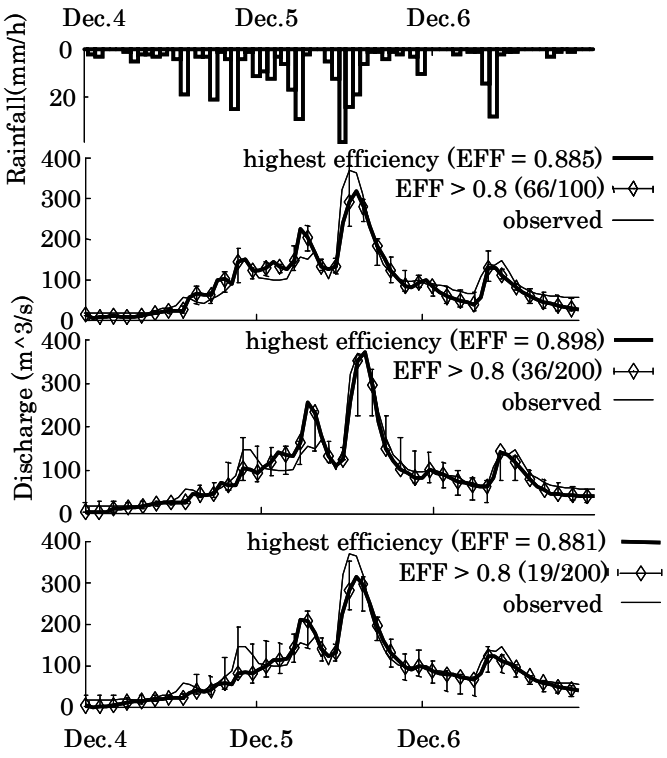

Fig. 3 Rainfall–runoff simulation for the calibration.

stable than Models 2 and 3. We define a Nash–Sutcliffe efficiency (EFF) of 0.8 as the threshold EI_*. As a result, the reliability ($\alpha_{ung}(0.8)$) of Model 1 is 66%, but only 18%

and 9.5% for Models 2 and 3, respectively. Figure 3 shows the hydrographs simulated with the three models. Each part of Fig. 3 shows the observed hydrograph and a simulated hydrograph of the highest efficiency uncertainty bands (Beven & Binley, 1992) representing the highest and lowest simulated hydrographs satisfying the threshold. Although Model 2 gives the highest efficiency in the simulations, Model 1 is more reliable for application to an ungauged basin with similar hydro-climatic condition to the Lesti River basin.

Since observed discharge data are available in the Lesti River basin, we estimate the model reliability for a gauged basin with rainfall–discharge sequences observed during 7–10 October 1992. This process regards vectors satisfying the threshold EI_* discussed previously as calibrated parameter vectors. We simulated the hydrograph with the calibrated parameter vectors for the validation period to obtain evaluation indices (EI_V). Figure 4 shows the relative frequency of EI_v. With a Nash-Sutcliffe efficiency (EFF) of 0.7 as a threshold (EI_{v*}), we obtained the reliability of the three models in the Lesti River basin. The reliability of Models 1, 2 and 3 was 0%, 36%, and 31%, respectively. Figure 5 shows the highest efficiency hydrographs and the uncertainty bands (the maximum and minimum ranges of hydrographs) simulated by the three models. Although the calibrated parameters are used, the uncertainty bands calculated by Models 2 and 3 are still wide. With regards to efficiency, Model 3 (EFF = 0.809) scores slightly higher than Model 2 (EFF = 0.792). However, we would say that Model 2 is more reliable when discharge data is available from the viewpoint of reliability.

Model uncertainties for sediment load predictions

Figure 6 shows sediment load results computed with the three models. The uncertainty bands denote the maximum and minimum sediment load simulated with the calibrated parameter vectors (EFF > 0.8). The uncertainty band of the sediment-load prediction (Fig. 6) is much larger than the uncertainty of rainfall–runoff simulation (Fig. 3), which implies that a calibration with discharge data is not sufficient to simulate sediment load accurately.

Sediment load simulation for the rainy season

Using the constructed model, we conducted a sediment load simulation for the Lesti River basin. The simulation period is the rainy season from November 1995 to April 1996. The parameter vector used here is the one that performed the best during the calibration period. Model 2 is used for this simulation because the reliability evaluation made it clear that this is the most reliable of the three models of the Lesti River basin. The factor for the Manning coefficient, hydraulic conductivity, and depth of subsurface layer are 0.64, 0.013 m s^{-1} and 55.3 cm, respectively.

Figure 7 shows the simulation results as, from top to bottom, a hyetograph, cumulative sediment load at the basin outlet, the riverbed elevation at the outlet, and the cumulative sediment yield from the whole basin. The cumulative sediment load at

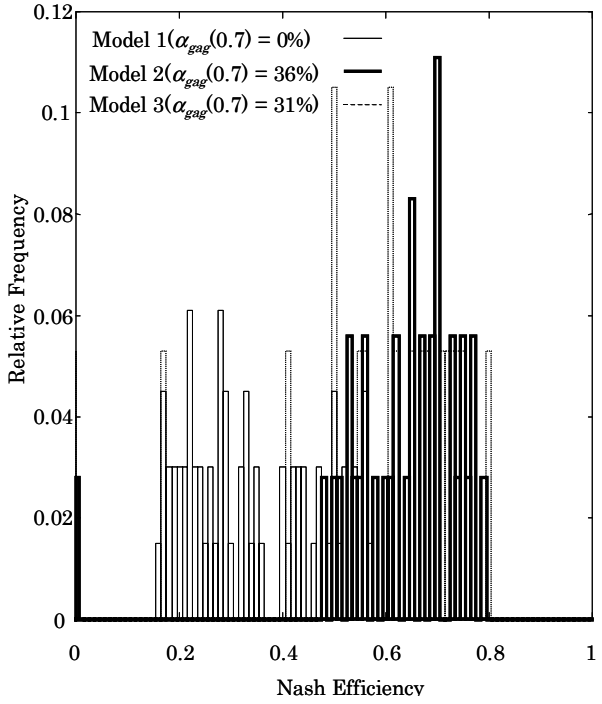

Fig. 4 Frequency distribution of Nash-Sutcliffe Efficiency for the validation.

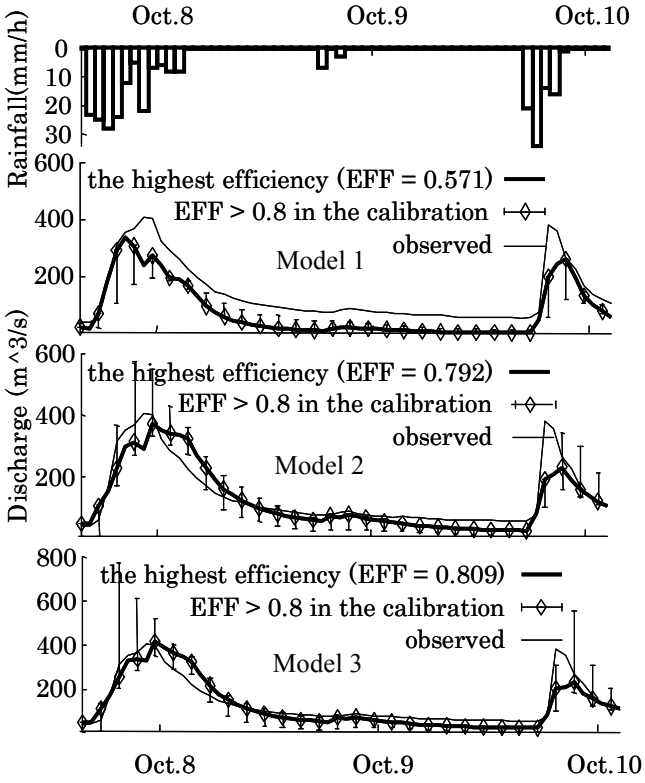

Fig. 5 Rainfall–runoff simulation for the validation.

the outlet is gradually increasing during the simulation period, while sediment is yielded in a short period. A severe storm from 4–6 December 1995 yielded more than

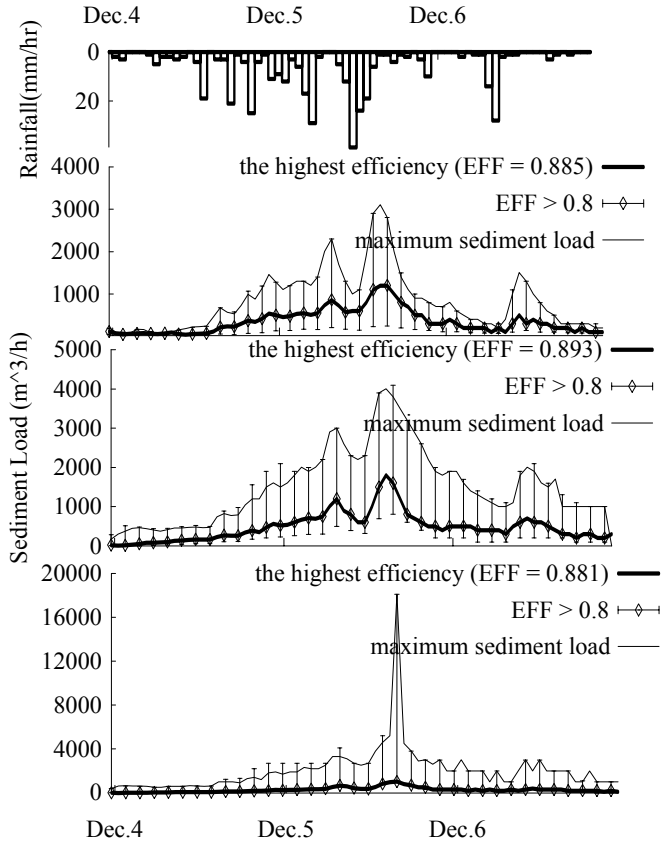

Fig. 6 Sediment-load simulation for the calibration.

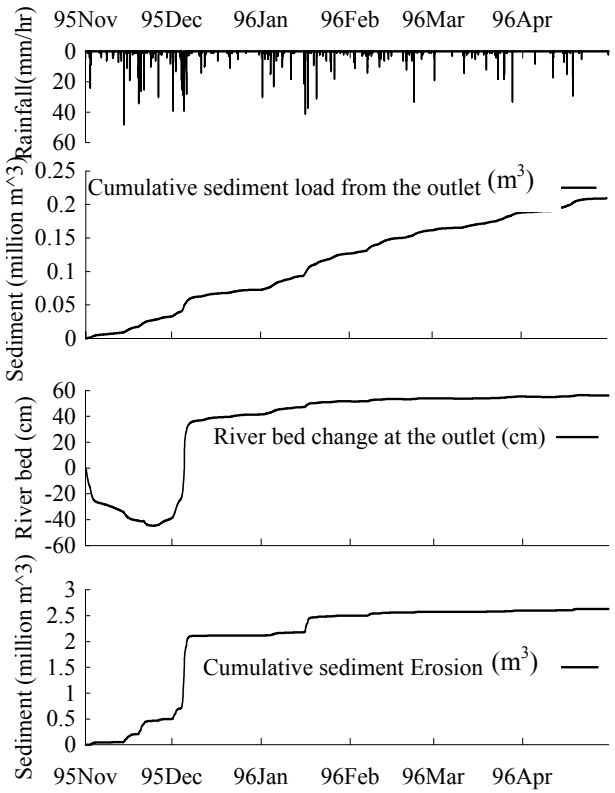

Fig. 7 Sediment simulation results for a rainy season by Model 2.

1×10^6 m^3 of sediment. The riverbed gradually degraded until the severe storm, but during the storm the riverbed aggraded by approximately 1 m within 3 days. After the storm, riverbed elevation increased slowly because sediment deposited upstream was gradually transported further downstream.

Figure 8 shows the evolution of the longitudinal profile. One month after the simulation starts (1 December 1995), the riverbed becomes smoother than the original. Two months later (1 January 1996), some depressions in the riverbed have been filled in with sediment because of the severe storm of 4–6 December. A large amount of eroded material from the hillslopes contributes to the aggradation of the riverbed. According to Fig. 6, only one tenth of the eroded sediment is transported to the basin outlet, whereas the rest is deposited on the riverbed. The assumption of equilibrium sediment transport theory is one of the reasons that large amounts of sediment are deposited in some depressions. Applying a nonequilibrium sediment transport model is expected to improve the accuracy of the sediment transportation simulation, since the model can deal with delayed sediment deposition.

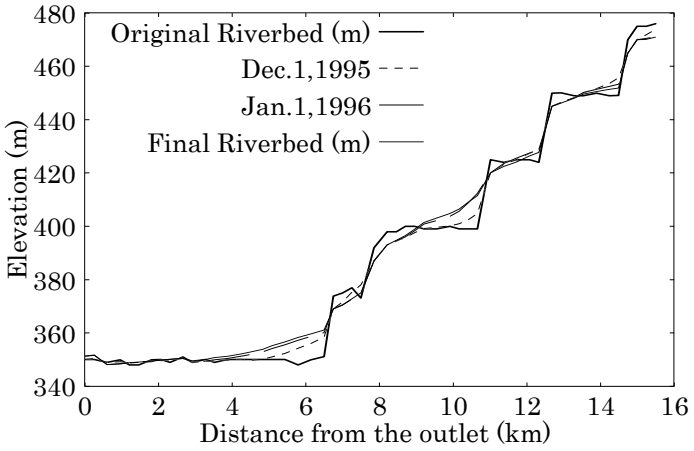

Fig. 8 Simulated riverbed evolution by Model 2.

CONCLUSIONS

In this paper we propose a method to evaluate model reliability by using a Monte Carlo simulation technique, and applied it to a distributed rainfall–sediment–runoff model. Accomplishments and results are summarized as follows:

(a) The rainfall–runoff model considers surface flow, subsurface flow, and field capacity. It simulates erosion based on the Unit Stream Power theory on slope grid-cells and sediment transport in river grid-cells.
(b) The proposed evaluation method can be used to investigate model reliability.
(c) The model with the calibrated parameters is used to simulate runoff and sediment load in the Lesti River basin, Indonesia. The uncertainty bands of the sediment load simulations are much wider than those of runoff simulations. To reduce the uncertainty, observed sediment data is indispensable.

(d) As a result of a simulation for a rainy season, we could confirm that the model can express the natural physical processes of sediment movement in such a way that a severe storm yields a large amount of sediment, and the sediment deposited on the riverbed is transported gradually further downstream.
(e) For future research, nonequilibrium sediment transport theory should be applied so that the model can account for the delay of sediment deposition.

REFERENCES

Ashida, K. & Michiue, M. (1972) Study on hydraulic resistance and bed-load transport rate in alluvial streams. *Proc. JSCE* **206**, 59–69.

Beven, K. J. & Binley, A. M. (1992) The future of distributed models: Model calibration and uncertainty prediction. *Hydrol. Processes* **6**, 279–298.

Kojima, T. (1997) Application of remote sensing and GIS to hydrological analysis. Doctorate of Engineering Dissertation, Kyoto University, Japan.

Lane, E. & Kalinske, A. A. (1941) Engineering calculation of suspended sediment. *Trans. Am. Geophys. U.* **22**, 603–607.

Moore, I. D. & Burch, G. J. (1986) Sediment transport capacity of sheet and rill flow. *Water Resour. Res.* **22**, 1350–1360.

NASDA (1997) *ADEOS Reference Handbook*. Development Service Co., LTD, Japan.

Nash, J. E. & Sutcliffe, J. V. (1970) River flow forecasting through conceptual models. Part I, A discussion of principles. *J. Hydrol.* **10**, 282–290.

Shiiba, M. *et al* (1998) Development of slope runoff models which consider field capacity and pipe flows. *Ann. Disaster Prevention Res. Inst.*, Kyoto University, **41**(b-2)**,** 229–235.

Takara, K. & Sayama, T. (2002) A physically-based rainfall–sediment–runoff model in a catchment scale—Application to the upper Brantas River basin, Indonesia. In: *Water Resources and Environment Research* (ed. by G. H. Schmitz) (Proc. Third ICWRER Dresden, Germany, July 2002), **2**, 256–261.

Yang, C. T. (1996) *Sediment Transport—Theory and Practice*. McGraw-Hill, New York, USA.